

Scenery from the Top: Study of the Third Generation Squarks at CERN LHC

Junji Hisano,^{1,2} Kiyotomo Kawagoe,³ Ryuichiro Kitano,^{2,4} and Mihoko M. Nojiri⁵

¹*ICRR, University of Tokyo, Kashima 277-8582, Japan*

²*IPNS, KEK, Tsukuba 305-0801, Japan*

³*Department of Physics, Kobe University, Kobe 657-8501, Japan*

⁴*Department of Physics, Tohoku University, Sendai 980-77, Japan*

⁵*YITP, Kyoto University, Kyoto 606-8502, Japan*

(Dated: January 23, 2003)

In the minimal supersymmetric standard model (MSSM) properties of the third generation sfermions are important from the viewpoint of discriminating the SUSY breaking models and in the determination of the Higgs boson mass. If gluinos are copiously produced at CERN LHC, gluino decays into tb through stop and sbottom can be studied using hadronic decays of the top quark. The kinematical endpoint of the gluino decays can be evaluated using a W sideband method to estimate combinatorial backgrounds. This implies that fundamental parameters related to the third generation squarks can be reliably measured. The top-quark polarization dependence in the decay process may also be extracted by looking at the b jet distribution near the kinematical endpoint.

PACS numbers: **12.60.Jv**, **14.80.Ly**

The minimal supersymmetric standard model (MSSM) is one of the promising extensions of the standard model (SM). The model requires superpartners of ordinary particles (sparticles), and LHC at CERN might confirm the existence of these new particles [1]. Since the sparticle masses are related to the SUSY breaking mechanism, measurement of the masses provides a way to probe the origin of SUSY breaking in nature.

The masses and mixings of stops ($\tilde{t}_{1,2}$) and sbottoms ($\tilde{b}_{1,2}$) are sensitive to the flavor structure of scalar masses. First, the diagonal masses in the stop and sbottom mass matrices, $m_{\tilde{Q}_3}$, $m_{\tilde{t}_R}$, and $m_{\tilde{b}_R}$, are predicted to be less than those of other squarks in the minimal supergravity (MSUGRA) model [2] because of the Yukawa RGE running effects. Some SUSY breaking models, such as the flavor U(2) model [3] or the decoupling solution [4], and the superconformal model [5] for the SUSY flavor problem, have also special imprints on these parameters. The \tilde{t}_L - \tilde{t}_R -Higgs trilinear coupling A_t at the weak scale has a large coefficient proportional to m_t , resulting in a large left-right mixing of stops: $m_{\tilde{t}_R}^2 = m_t(A_t - \mu \cot \beta)$. In the MSUGRA A_t is proportional to the universal gaugino mass M at the GUT scale M_{GUT} , and insensitive to the A parameter at M_{GUT} [6]. Indeed, this is one of the robust predictions of SUSY breaking at M_{GUT} . These relations is not guaranteed if the SUSY breaking mediation scale is much smaller than M_{GUT} . It should be stressed that the stop masses and the mixing are very important parameters to predict the light Higgs mass [7].

It is possible to study the stop and sbottom at LHC through the gluino (\tilde{g}) decay modes listed below.

$$\begin{aligned}
 \text{I)} & \quad \tilde{g} \rightarrow \tilde{b}b_1 \rightarrow \tilde{b}b\tilde{\chi}_2^0 \rightarrow \tilde{b}b\tilde{t}\tilde{t}^-\tilde{\chi}_1^0, \\
 \text{II)} & \quad \tilde{g} \rightarrow \tilde{t}t_1^* \rightarrow \tilde{t}t\tilde{\chi}_1^0, \\
 \text{III)} & \quad \tilde{g} \rightarrow \tilde{t}t_1^* \rightarrow \tilde{t}b\tilde{\chi}_1^\pm, \\
 \text{IV)} & \quad \tilde{g} \rightarrow \tilde{b}b_1 \rightarrow \tilde{t}b\tilde{\chi}_1^\pm.
 \end{aligned}
 \tag{1}$$

In previous literatures [1, 8], the third generation sfermions are often studied using the mode I) ($\tilde{b}b\tilde{t}\tilde{t}^-$ channels). This mode is important when $\tilde{\chi}_2^0$ has substantial branching ratios into leptons. Measurement of the kinematical endpoints of the signal distributions tells us the sparticle masses. Unfortunately, the branching ratios could be very small, and this mode is insensitive to the stop. We tried to study the mode II) in Eqs. (1), but the result was unsuccessful because of the small branching ratio in the MSUGRA.

In this paper we try to measure the endpoints of the modes III) and IV) in Eqs. (1). The decay modes are expected to be dominant in the MSUGRA since $\tilde{\chi}_1^\pm$ is likely to be SU(2)_L gaugino-like and $Br(\tilde{b}_1, \tilde{t}_1 \rightarrow \tilde{\chi}_1^\pm)$ could be as large as 60%. We focus on the reconstruction of hadronic decay of the top quark, because the distribution of the tb invariant mass m_{tb} makes a clear endpoint in this case.

The parton level distribution of the tb final state invariant mass is expressed as a function of $m_{\tilde{g}}$, $m_{\tilde{t}_1}$, $m_{\tilde{b}_1}$, and chargino mass $m_{\tilde{\chi}_1^\pm}$: $d\Gamma/dm_{tb} \propto m_{tb}$, and the endpoints M_{tb} for the modes III) and IV) are written as follows;

$$\begin{aligned}
 M_{tb}^2 \text{ (III)} &= m_{\tilde{t}_1}^2 + \frac{m_{\tilde{t}_1}^2 - m_{\tilde{\chi}_1^\pm}^2}{2m_{\tilde{t}_1}^2} \left\{ (m_{\tilde{g}}^2 - m_{\tilde{t}_1}^2 - m_{\tilde{t}_1}^2) \right. \\
 & \quad \left. + \sqrt{(m_{\tilde{g}}^2 - (m_{\tilde{t}_1} - m_t)^2)(m_{\tilde{g}}^2 - (m_{\tilde{t}_1} + m_t)^2)} \right\}, \\
 M_{tb}^2 \text{ (IV)} &= m_{\tilde{t}_1}^2 + \frac{m_{\tilde{g}}^2 - m_{\tilde{b}_1}^2}{2m_{\tilde{t}_1}^2} \left\{ (m_{\tilde{t}_1}^2 - m_{\tilde{\chi}_1^\pm}^2 + m_{\tilde{t}_1}^2) \right. \\
 & \quad \left. + \sqrt{(m_{\tilde{g}}^2 - (m_{\tilde{t}_1} - m_t)^2)(m_{\tilde{g}}^2 - (m_{\tilde{t}_1} + m_t)^2)} \right\}.
 \end{aligned}$$

Note that the endpoint of the final state $\tilde{t}b\tilde{\chi}_1^\pm$ should be sensitive to both \tilde{t}_1 and \tilde{b}_1 .

In order to demonstrate the endpoint reconstruction, we take an MSUGRA point with the scalar mass $m =$

	$m_{\tilde{g}}$	$m_{\tilde{t}_1}$	$m_{\tilde{b}_1}$	$m_{\tilde{b}_2}$	σ		$m_{\tilde{g}}$	$m_{\tilde{t}_1}$	$m_{\tilde{b}_1}$	$m_{\tilde{b}_2}$	σ
A1	707	427	570	613	26	A2	706	496	587	614	25
G1	807	427	570	613	18	G2	806	496	587	614	18
T1	707	327	570	613	30	T2	707	477	570	612	25
B	609	402	504	534	56	C	931	636	771	805	5
G	886	604	714	763	7	I	831	571	648	725	10
E1	515	273	521	634	77	E2	747	524	770	898	8

TABLE I: The particle masses in GeV and the total SUSY cross sections in pb for the parameter points studied in this paper.

100GeV, the gaugino mass $M = 300\text{GeV}$, the A parameter -300GeV at the GUT scale, $\tan\beta = 10$ and $\mu > 0$. This corresponds to the sample point A1 in Table 1. The masses and mixings of sparticles are calculated by ISASUSY/ISASUGRA [9]. The Monte Carlo SUSY events are generated by PYTHIA [10] using the masses and mixings, and then passed through a fast detector simulation program for the ATLAS experiment [11]. Jets are reconstructed by a cone-based algorithm with $\Delta R = 0.4$. The b and τ tagging efficiencies are set to be 60% and 50%, respectively.

In our study we apply the following selection for the tb signal; 1) $E_T^{\text{miss}} > 200$ GeV, 2) $m_{\text{eff}} > 1000$ GeV ($m_{\text{eff}} = E_T^{\text{miss}} + \sum_{\text{all}} p_T^{\text{jet}}$), 3) two and only two b -jets with $p_T > 30$ GeV, 4) $4 \leq n_{\text{jet}} \leq 6$ (n_{jet} , number of additional jets with $p_T > 30$ GeV and $|\eta| < 3.0$). In addition, events with leptons are removed to reduce the background from $t\bar{t}$ production. At this stage the number of remaining $t\bar{t}$ events is rather small, about 10% of the remaining SUSY events for the point A1.

To reconstruct the hadronic decay of the top quark, we first take a jet pair consistent with a hadronic W boson decay with a cut on the jet pair invariant mass m_{jj} ; $|m_{jj} - m_W| < 15\text{GeV}$. The invariant mass of the jet pair and one of the b jets, m_{bjj} , is then calculated. All possible combinations are tried in an event, and the combination which minimizes $|m_{bjj} - m_t|$ is chosen. The jet combination is regarded as a top candidate if $|m_{bjj} - m_t| < 30\text{GeV}$. The energy and momentum of the jet pair are then rescaled so that $m_{jj} = m_W$.

The expected tb endpoint is not clearly visible in the m_{tb} distribution shown in Fig. 1(a). As there are 7 to 8 jets on average in a selected event, events with a fake W boson (and a fake top quark) dominate the distribution. The distribution of the fake W events is estimated from the events that contain jet pairs with the invariant mass in the ranges A) $|m_{jj} - (m_W - 15\text{GeV})| < 15$ GeV and B) $|m_{jj} - (m_W + 15\text{GeV})| < 15$ GeV; ‘the W sidebands’. The energy and momentum of the jet pairs are then rescaled linearly to be in the range $|m_{jj} - m_W| < 15\text{GeV}$. The fake top candidates are reconstructed from the rescaled jet pairs and b jets in the events.

The estimated background distribution is shown in

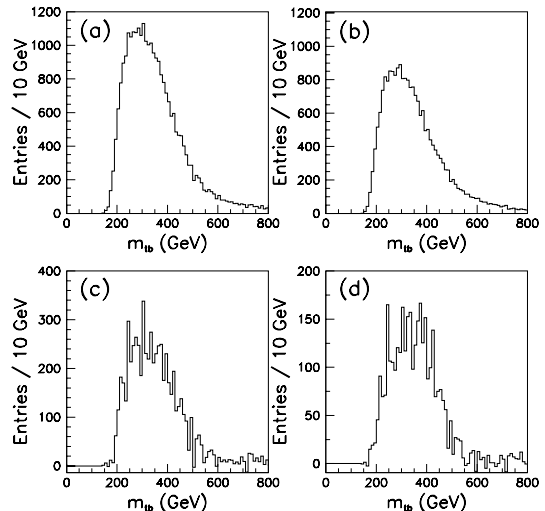


FIG. 1: (a) The signal m_{tb} distribution for the sample point A1 in Table 1, (b) the estimated background distribution from the sideband events, (c) (a)–(b), and (d) the m_{tb} distribution for the modes III) and IV) in Eqs. (1), and a decay mode irreducible to the mode III).

Fig. 1(b), which is obtained by averaging distributions from the sidebands A) and B). The estimation is based on an assumption that most of the jets in the events do not have significant correlation with the b jets in the events. The estimated background distribution is subtracted from the signal distribution in Fig. 1(c). The estimated *correct* signal distribution (c) shows the better endpoint compared to (a). Fig. 1(d) is the same distribution as Fig. 1(c) but for the events which contain the mode III), the mode IV), or a decay mode irreducible to the mode III); $\tilde{g} \rightarrow \tilde{b}_1 b \rightarrow \tilde{t}_1(Wb) \rightarrow b\tilde{\chi}_1^-(bW)$. Note that if (bW) has an invariant mass consistent to a top, the decay is kinematically equivalent to the mode III). Fig. 1(d) shows the expected clear edge at the right place ($M_{tb}(\text{III}) = 476\text{GeV}$ and $M_{tb}(\text{IV}) = 420$ GeV), demonstrating that the sideband method works well. Here, the number of the generated SUSY events is 3×10^6 , which corresponds to an integrated luminosity of 120fb^{-1} . The plots do not include the SM backgrounds.

Note that the signals from the modes III) and IV) in Eqs. (1) are significant in the total selected events. We fit the total distribution shown in Fig. 1(c) by a simple fitting function, which is described as a function of the endpoint M_{tb}^{fit} , the edge height h , and the smearing parameter σ from the jet energy resolution. We assume that the signal distribution is sitting on a linearly-decreasing background. The M_{tb}^{fit} is compared with the weighted endpoint M_{tb}^w defined by

$$M_{tb}^w = \frac{Br(\text{III})M_{tb}(\text{III}) + Br(\text{IV})M_{tb}(\text{IV})}{Br(\text{III}) + Br(\text{IV})},$$

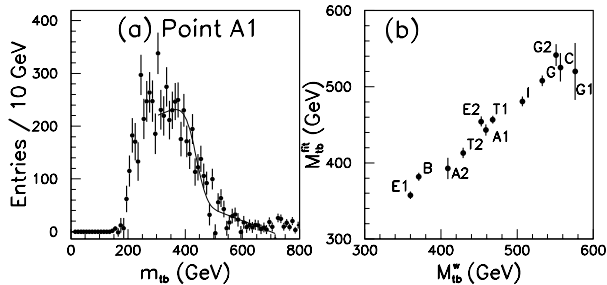


FIG. 2: (a) A fit to the m_{tb} distribution (point A1), and (b) comparison of M_{tb}^{fit} and M_{tb}^w for the sample parameters given in this paper.

where $Br(\text{III})$ and $Br(\text{IV})$ are branching ratios for the modes III) and IV), respectively. The fit is shown in Fig. 2 (a). We obtain $M_{tb}^{\text{fit}} = 443.2 \pm 7.4$ GeV, which is consistent with $M_{tb}^w = 459$ GeV. The M_{tb}^{fit} changes moderately when one changes the m_{tb} range used for the fit. We choose the range so that the significance of the height $S = h/\Delta h$ is at maximum. For the fit shown in Fig. 2(a), $S(\text{max}) = 196.9/15.2 = 13.0$ is obtained.

In order to check the availability of the endpoint measurement, we study twelve sample points in total, including the previous point, shown in Table 1, and compare M_{tb}^{fit} and M_{tb}^w . We choose two reference MSUGRA points as A1 and A2, where $m = 100$ GeV, $M = 300$ GeV, $\tan\beta = 10$, $\mu > 0$ and $A = \mp 300$ GeV. We also study points with different mass spectrums from the MSUGRA predictions; two points with gluino masses heavier than the reference points, (G1, G2), and two points with modified stop masses (T1, T2). Furthermore, we include the MSUGRA points selected from [12] (B, C, G, I) and two non-SUGRA points E1 and E2 where the gluino decays exclusively into \tilde{t}_1 . The result is summarized in Fig. 2 (b)[14]. The error bars represent the statistical errors for 3×10^6 SUSY events at each point, and the systematic error of the jet energy scale (1%) is not included (see Table 1 for SUSY cross sections). This plot shows an impressive linearity between the expectation and the MC fits, although M_{tb}^{fit} is systematically lower than M_{tb}^w . This is reasonable since some of particles are always out of the cone to define jets. This effect may be corrected by comparing distributions with different jet definitions.

Another uncertainty may come from the jet fragmentation. If events are generated by ISAJET for the point A1, the reconstructed endpoint is smaller by 10%, and the number of events after the sideband subtraction is smaller by a factor of 1.5. The difference comes from the different jet fragmentation schemes. ISAJET radiates more soft jets for a parton, resulting in more background and smeared endpoint distribution. The event generators must be tuned carefully to extract the kinematical

information from the signal distribution.

We now discuss the physics that might be studied with the tb endpoint measurement.

We cannot determine all of the relevant mass parameters from only the tb endpoint measurement, since the endpoint M_{tb} depends on $m_{\tilde{g}}$, $m_{\tilde{b}_1}$, and $m_{\tilde{t}_1}$. Thus, the study of bbl^+l^- final state would be important to single out the possible \tilde{t} and \tilde{b} contributions to the tb final state and to proceed to a model-independent study. For example, let us assume that errors of the endpoints M_{bbl} and M_{bll} are 10 GeV and that of the endpoint $M_{b_{1l}}$ is 30 GeV in the measurement. Here, b_1 is one of the two b jets for which the invariant mass $m_{b_{1l}}$ is larger. When we generate $m_{\tilde{g}}$, $m_{\tilde{b}_1}$, $\tilde{\chi}_2^0$, and $\tilde{\chi}_1^0$ randomly around the reference point A1 fixing the endpoint M_{ll} (which is expected to have a very small error), and require $\Delta\chi^2 \equiv \sum_i (M_i - M_i^{A1})^2 / \Delta M_i^2 < 1(9)$ (i runs over the possible endpoints), the deviation $M_{tb}(\text{IV}) - M_{tb}^{A1}(\text{IV})$ is always less than 15(45) GeV. For the point A1, $M_{tb}(\text{IV}) = 420$ GeV and $M_{tb}^w \sim 460$ GeV. The difference of $M_{tb}(\text{IV})$ and M_{tb}^w therefore may be statistically distinguishable.

The measurement of the SUSY breaking parameters in different sectors might reveal an overall inconsistency of the SUSY breaking mediation models. The distribution of the invariant mass formed by combining the highest P_T jet and a same-flavor and opposite-sign lepton pair (jll channels) is sensitive to $m_{\tilde{q}}$ and $m_{\tilde{l}}$, and this may lead to the determination of m and M in the MSUGRA [1, 13]. Once M and m are fixed, they strongly constrain the endpoint M_{tb}^w in the MSUGRA – by comparing it with the measured value, one should be able to check if $m_{\tilde{q}}$ or $m_{\tilde{l}}$ are consistent to the MSUGRA predictions.

Note also that the formulae of M_{tb} or M_{bbl} involve $m_{\tilde{g}}$, while the first generation squark mass is lower bounded by $m_{\tilde{g}}$ in the model. If $m_{\tilde{g}} \gg m_{\tilde{q}}$ is established by combining the squark mass scale determined through a jll analysis [1] and the analysis of the final state involving b jets, we can show that some new physics should occur below the scale where $m_{\tilde{q}}^2 < 0$. Note that, in the points G1 and G2 in Table 1, where the gluino mass is increased by 100 GeV from the MSUGRA predictions, m^2 becomes negative at the GUT scale. We study the jll distributions for the point G2 in a similar way as given in Ref. [13] and find that the jll endpoints are successfully reconstructed. Therefore the information on $m_{\tilde{q}}$ should be obtained in this case.

In the framework of the MSUGRA, the measurement of M_{tb} is sensitive to the GUT scale A parameter. This effect is large when $M \times A < 0$ as can be seen in Fig. 3. Here we take $M \sim m$ and $m = 230$ GeV, and vary A so that $|A| < 3m$. The M_{tb}^w and $m_{\tilde{t}_1}$ vary by 50 GeV and 150 GeV, respectively, and the changes are again detectable. Note that the $\tilde{\chi}_2^0$ decay into $\tilde{l}l$ is closed in this case, therefore the information from the bbl^+l^- channels is not available. If $m = 100$ GeV and A is varied from -300 GeV to 300 GeV, M_{tb}^w and $m_{\tilde{t}_1}$ change by 30 GeV

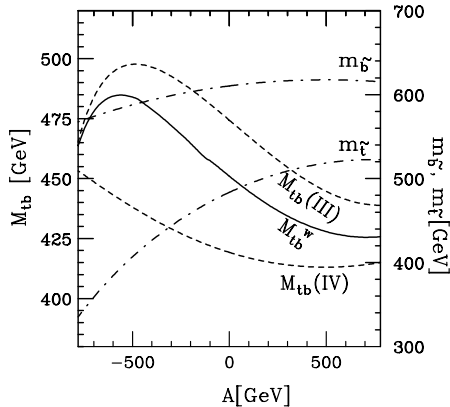


FIG. 3: Dependence of M_{tb} , $m_{\tilde{t}_1}$, and $m_{\tilde{b}_1}$ on the GUT scale A parameter in the MSUGRA.

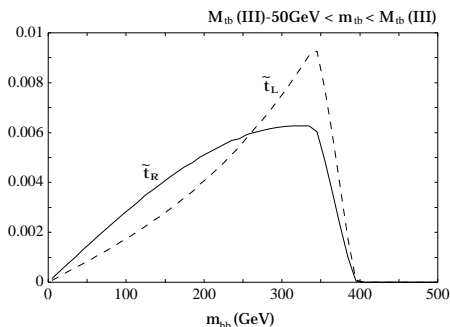


FIG. 4: The parton level distribution of m_{bb} for point A1. The two histograms show the distribution for the event with $M_{tb}(\text{III}) - 50\text{GeV} < m_{tb} < M_{tb}(\text{III})$ in cases $\tilde{t}_1 = \tilde{t}_R$ and $\tilde{t}_1 = \tilde{t}_L$.

and 70 GeV, respectively.

Finally, we discuss top-quark polarization dependence in the gluino decay. Naturally all top quarks coming from \tilde{g} , \tilde{t}_1 , and \tilde{b}_1 decays are polarized, depending on the sfermion and chargino mixings. For example, when \tilde{t}_1 is mostly right(left)-handed stop, t of $\tilde{g} \rightarrow t\tilde{t}_1^*$ is $t_{R(L)}$. This propagates into the average top-quark helicity, if the top quark is relativistic enough in the gluino rest frame. If the tb invariant mass is close to the endpoint M_{tb} of the mode III) in Eqs. (1), the t and b go to the opposite direction in the gluino rest frame. Because the bottom quark from the top-quark decay tends to go to the opposite direction to the top-quark helicity, the distribution of the invariant mass m_{bb} for events with m_{tb} close to $M_{tb}(\text{III})$ depends on the average top-quark helicity. The parton-level distributions of m_{bb} are plotted in Fig. 4 for the point A1. The solid (dotted) curve shows the distribution for the events with $M_{tb}(\text{III}) - 50\text{GeV} < m_{tb} < M_{tb}(\text{III})$ in the case of $\tilde{t}_1 = \tilde{t}_R$ ($\tilde{t}_1 = \tilde{t}_L$). One can read from Fig. 1 that roughly 200 signal events are available near the endpoint. The statistical difference between the two distributions is 3σ for 100 signal events without taking care of the background [15].

In this paper, we try to reconstruct final states which consisting of hadronic jets at LHC. This was considered difficult due to the large combinatorial background, but is overcome by a W sideband method developed to estimate the background. We reconstruct the $t\bar{b}$ final state from the event containing two b jets. The reconstructed endpoint provides us an access to the gluino and the third generation sparticle masses without relying on the decay modes including leptons. The correct reconstruction of the events also allows us to consider the top-quark polarization dependence of the distribution. This information is important to determine the radiative correction to the Higgs mass, as well as the origin of SUSY breaking.

It is a pleasure to thank Dr. Kanzaki and Mr. Toya for the construction of a simulation environment. We acknowledge ICEPP, Univ. of Tokyo, for providing us computing resources. This work is supported in part by the Grant-in-Aid for Science Research, Ministry of Education, Science and Culture, Japan (No. 12047127 for MMN).

-
- [1] ATLAS: Detector and physics performance technical design report, CERN-LHCC-99-14.
 - [2] See references in H. P. Nilles, Phys. Rept. **110**, 1 (1984).
 - [3] R. Barbieri, G. R. Dvali and L. J. Hall, Phys. Lett. B **377**, 76 (1996).
 - [4] See references in J. Hisano, K. Kurosawa and Y. Nomura, Phys. Lett. B **445**, 316 (1999).
 - [5] A. E. Nelson and M. J. Strassler, JHEP **0009**, 030 (2000); T. Kobayashi, H. Nakano, T. Noguchi and H. Terao, hep-ph/0202023.
 - [6] M. Carena and C. E. Wagner, Nucl. Phys. B **452**, 45 (1995).
 - [7] H. E. Haber and R. Hempfling, Phys. Rev. Lett. **66**, 1815 (1991); Y. Okada, M. Yamaguchi and T. Yanagida, Prog. Theor. Phys. **85**, 1 (1991); J. R. Ellis, G. Ridolfi and F. Zwirner, Phys. Lett. B **257**, 83 (1991); R. Barbieri and M. Frigeni, Phys. Lett. B **258**, 395 (1991).
 - [8] I. Hinchliffe, F. E. Paige, E. Nagy, M. D. Shapiro, J. Soderqvist and W. Yao, LBNL-40954.
 - [9] H. Baer, F. E. Paige, S. D. Protopopescu and X. Tata "ISAJET 7.48: a Monte Carlo event generator for pp , $p\bar{p}$, and e^+e^- reactions", hep-ph/0001086.
 - [10] T. Sjostrand, L. Lonnblad and S. Mrenna "PYTHIA 6.2: physics and manual", hep-ph/0108264.
 - [11] E. Richter-Was et al., ATLFAST2.21, ATLAS Internal Note PHYS-NO-079.
 - [12] M. Battaglia et al., Eur. Phys. J. C **22**, 535 (2001).
 - [13] H. Bachacou, I. Hinchliffe and F. E. Paige, Phys. Rev. D **62**, 015009 (2000).
 - [14] For the point C where SUSY decays contain many leptons, we omit the lepton veto and reduce the $t\bar{t}$ background by requiring $m_{bl} > 140$ for any lepton with $p_T > 10$ GeV.
 - [15] For events with $m_{tb} < M_{tb}(\text{III}) - 50$ GeV the gluino decay into \tilde{b}_1 starts to contribute.